

Stabilizer Entropy and entanglement complexity in the Sachdev-Ye-Kitaev model

Barbara Jasser^{1,2}, Jovan Odavić^{2,3}, and Alioscia Hamma^{1,2,3}

¹*Scuola Superiore Meridionale, Largo S. Marcellino 10, 80138 Napoli, Italy*

²*Istituto Nazionale di Fisica Nucleare (INFN), Sezione di Napoli, Italy and*

³*Dipartimento di Fisica ‘Ettore Pancini’, Università degli Studi di Napoli Federico II, Via Cintia 80126, Napoli, Italy*

The Sachdev-Ye-Kitaev (SYK) model is of paramount importance for the understanding of both strange metals and a microscopic theory of two-dimensional gravity. We study the interplay between Stabilizer Rényi Entropy (SRE) and entanglement entropy in both the ground state and highly excited states of the SYK4+SYK2 model interpolating the highly chaotic four-body interactions model with the integrable two-body interactions one. The interplay between these quantities is assessed also through universal statistics of the entanglement spectrum and its anti-flatness. We find that SYK4 is indeed characterized by a complex pattern of both entanglement and non-stabilizer resources while SYK2 is non-universal and not complex. We discuss the fragility and robustness of these features depending on the interpolation parameter.

Introduction.— The Sachdev-Ye-Kitaev (SYK) model [1, 2] describes the behavior of strongly correlated fermions in strange metals [3]. In recent years, the model has gained new interest from the high-energy community due to its holographic duality [4–6]. In the infra-red limit and large number of degrees of freedom, the model acquires conformal symmetry. The leading corrections to the out-of-time-ordered four-point correlation functions exhibit exponential growth over time. The rate of this growth reaches the universal upper bound established in [7], see [8, 9]. The low-energy sector of the SYK4 model is governed by an emergent reparametrization symmetry, described by Jackiw-Teitelboim (JT) gravity [6], providing insight into the holographic description of black holes and their thermodynamic properties.

The interpolation between the four-body (SYK4) and the two-body (SYK2) model [10, 11] provides a connection to a model of strongly correlated electrons. The two theories are very different: the SYK4 is chaotic, with an exponential density of states at low energy, while the SYK2 is integrable, with a polynomially vanishing gap. Remarkably, both models exhibit a volume law for entanglement. One wonders what makes these two regimes so different. Entanglement has been deeply investigated to better understand both the chaotic nature of SYK models [12–14] and their connection to holographic theory and complex quantum systems [3, 15, 16] but the transition to SYK2 shows that entanglement alone is not enough.

The second layer of quantum complexity is given by non-stabilizerness [17], a crucial resource in the context of universal quantum computation, error correction [18–22] and quantum simulation [23–26]. Recently, non-stabilizerness has risen to prominence due to finding a unique computable monotone for pure states, the Stabilizer Rényi Entropy (SRE) [27]. In the context of high-energy physics, both SRE and entanglement are studied for heavy nuclei simulations [28] and neutrino physics [29, 30]. Moreover, the delocalization due to the entanglement of non-stabilizerness resources has recently been connected to the holographic dual of back-reaction in the context of AdS-CFT [31], features of CFT [32, 33], and the harvesting of quantum resources from the vac-

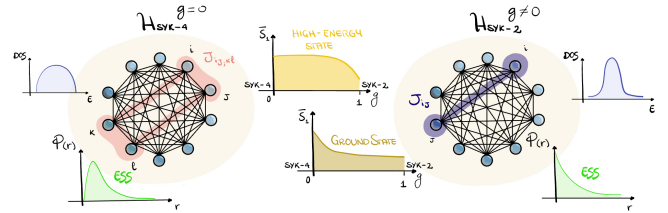


FIG. 1. Schematic representation of the SYK₄+SYK₂ model. The left side ($g = 0$) corresponds to SYK₄ with a semicircular Hamiltonian spectrum and Wigner-Dyson entanglement statistics. On the right side ($g = 1$) the SYK₂ model, exhibiting Poisson-like level statistics and lower entanglement complexity. The middle panels show the average entanglement \bar{S}_1 , one of the several figures of merit capturing the change in complexity.

uum of a quantum field [34, 35]. When entanglement delocalizes and scrambles non-stabilizer resources, this gives rise to universal behavior of out-of-time-order correlation functions, entanglement fluctuations [36, 37] and the onset of chaotic behavior in quantum many-body systems [38, 39] in the ETH-MBL transition [40–43]. On the other hand, the fine structure of entanglement revealed by the statistics of entanglement gaps (ESS) [39, 44, 45] reaches the complex universal patterns of random matrix theory thanks to non-stabilizerness.

The main goal of this Letter is to study the SYK4+SYK2 model beyond perturbative limits under the lens of the emergence of quantum complex behavior. As we shall see, this happens as a result of the interplay between entanglement and SRE. We find that SYK4 exhibits a complex interplay of entanglement and SRE both in the ground state and in the high-energy eigenstates (middle of the spectrum), while SYK2 shows patterns of this interplay that are typical of integrable or non-chaotic models. This is revealed by the adherence of SYK4 to Haar-like behavior for entanglement entropy, entanglement eigenvalues, and gaps statistics, capacity of

entanglement, higher values of SRE, especially in its non-local features. On the other hand, SYK2 shows a lower level of SRE, and non universal statistics in all the figures of merit mentioned above. An important question is how robust are these behaviors in the SYK4+SYK2 model. Mostly, SYK4 is fragile: a however weak perturbation by SYK2 will disrupt the universal features of the model. Remarkably, though, some features of the entanglement spectrum are very robust: the entanglement entropy, the statistics of the entanglement eigenvalues and the capacity of entanglement are robust features for the highly excited states: every perturbation of SYK2 will drive the system to the universal behavior of SYK4. These findings enrich those of [10] based on Green's functions. In addition, we also show that adherence to the energy spectrum to Wigner-Dyson universal behavior is fragile for SYK4+SYK2. Finally, we show that the behavior of SRE in the ground state is capable of classifying the 8-fold way of the symmetries of SYK4. A similar conclusion is also shown for the energy gap above the ground state. In order to argue about the robustness of these features, we apply quantum-information theoretic tools like the Kullback-Leibler divergence fidelity.

The model.— The most general form of SYK models [4, 46] considers a q -body all-to-all interaction between N_f Majorana fermionic modes. The Hamiltonian in terms of Majorana operators reads

$$H_q = (i)^{q/2} \sum_{1 \leq i_1 < \dots < i_q \leq N} J_{i_1 i_2 \dots i_q} \chi_{i_1} \chi_{i_2} \dots \chi_{i_q} \quad (1)$$

with q an even integer number. The disorder in the model is due to the couplings J_{i_1, i_2, \dots, i_q} which are identical, independent distributed (i.i.d.) gaussian variables with vanishing mean and variance

$$\overline{J_{i_1, i_2, \dots, i_q}} = 0; \quad \overline{J_{i_1, i_2, \dots, i_q}^2} = \frac{(q-1)! J}{N^{q-1}}. \quad (2)$$

For $q > 2$, the system exhibits quantum chaos [47, 48], as evidenced by several established indicators. One key probe is level repulsion in the energy spectra, characterized by the statistical distribution of energy level spacings [49–52]. This indicates that the eigenstates of the Hamiltonian are highly delocalized and correlated, a hallmark of quantum chaos. The system is defined on a complete graph, so the interactions are strongly non-local. Using the Jordan-Wigner transformations it is possible to map the Majorana operators into Pauli spin strings, used in the numerical simulations [53]. Notice that each spin operator can be expressed in terms of two Majorana operators. Therefore, the total number of Majorana operators is double the number of Paulis. The simplest version of SYK models is the SYK2

$$H_2 = i \sum_{1 \leq i < j \leq N} J_{i,j} \chi_i \chi_j. \quad (3)$$

Since the interactions between fermions are considered in pairs, SYK2 represents the free fermions point of the

theory. This results in Gaussian statistics for its spectral properties, meaning that it does not show the same level of randomness and complexity found in chaotic systems [5, 54]. The SYK2 model serves as a simple example of a disordered fermionic system and is analytically solvable [14]. The four-body interaction model, called SYK4, is

$$H_4 = - \sum_{1 \leq i < j < k < l \leq N} J_{i,j,k,l} \chi_i \chi_j \chi_k \chi_l. \quad (4)$$

This model satisfies the usual probes of quantum chaos [47, 48], i.e. the Hamiltonian exhibits level repulsion in its spectrum. The SYK4+SYK2 model is defined as [10]

$$H_g := (1-g)H_4 + gH_2, \quad (5)$$

with $g \in [0, 1]$. In the following, we compute by exact diagonalization the energy spectrum of H_g together with the exact ground state (GS) and middle-spectrum eigenstate (MS) for a number of realization M of the disorder. The eigenvalues of the reduced density operator (RDM) to half-system ρ_R will be denoted by $\{\lambda_k\}$ and are sorted in ascending order.

Entanglement.— To quantify the bipartite entanglement of the ground state of the SYK model, we focus on Rényi entropies defined as

$$S_\alpha = \frac{1}{1-\alpha} \log \text{Tr} [\rho_R^\alpha], \quad \alpha \in [0, 1) \cup (1, \infty), \quad (6)$$

The von Neumann entanglement entropy $S(\rho_R)_1 = -\text{Tr}(\rho_R \log(\rho_R))$ corresponds to the limit $\alpha \rightarrow 1^+$.

For random quadratic Hamiltonians, a class of models to which the SYK2 Hamiltonian belongs [14], the average ground-state entanglement entropy was derived in closed form in [55], given by

$$S_1^{\text{SYK2}}(R, f) = \mathcal{K}(f) \ln(2)R, \quad (7)$$

where

$$\mathcal{K}(f) = \left[1 - \frac{1 + f^{-1}(1-f) \ln(1-f)}{\ln 2} \right]. \quad (8)$$

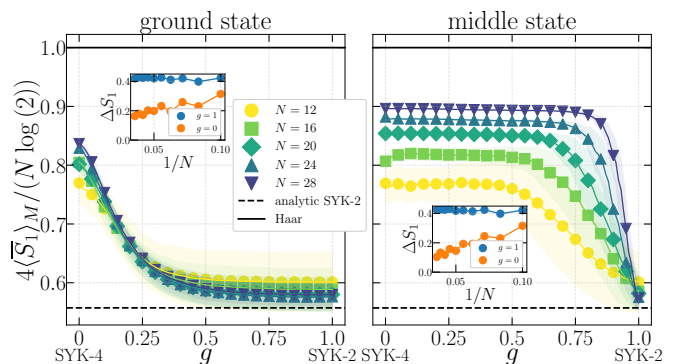


FIG. 2. Averaged bipartite entanglement in the GS (left panel) and MS (right panel) of the SYK4+SYK2 model H_g as a function of g . Shaded areas represent the standard deviation across M realizations of the Hamiltonian. The inset shows the finite size scaling of the relative gap ΔS_1 for $g = 0, 1$.

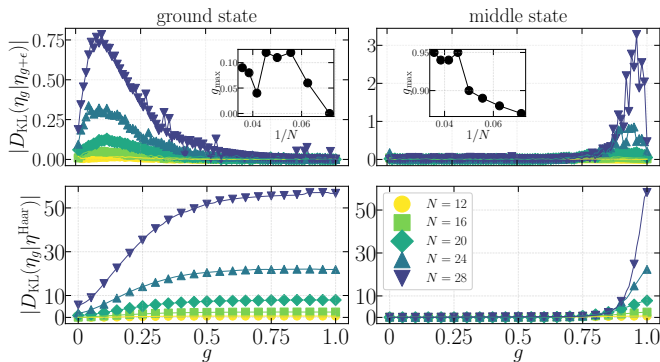


FIG. 3. Renormalized RDM eigenvalues as $\eta_k = k/d$ and $x_k = (1/2)\sqrt{p_k d}$ where $d = 2^{N/4}$ for $f = 1/2$. The reference value is the M-P distribution $\eta^{\text{Haar}}(x)$.

Here, $f = R/N$ represents the ratio between the subsystem size R and the total system size N in terms of the number of qubits. The entanglement entropy scaling of the SYK2 ground state follows a volume law (extensive scaling with subsystem size) but with a coefficient dependent on the ratio f , distinguishing it from the fully quantum chaotic regime in the thermodynamic limit.

Efforts to extend these insights to the SYK4 model include works such as Refs. [12, 56, 57]. On the other hand, the maximally chaotic random pure state, sampled uniformly according to the Haar measure, exhibits the Page value for entanglement entropy, given by

$$\frac{2S_1^{\text{Haar}}}{N \ln(2)} = 2f, \quad \text{for } f \in [0, 1/2], \quad (9)$$

to leading order in the system size [58, 59].

In Fig. 2, we present the results for the rescaled entanglement entropy in the GS and MS of H_g of the interpolated SYK Hamiltonian, with $f = 1/2$. The averaging is performed over different partitions of the system (denoted with an overline \bar{S}) and multiple realizations (denoted with $\langle \rangle_M$) of the model for each value of the interpolation parameter g . Details of the realization and disorder statistics for various system sizes are provided in [60]. We define $\Delta S_1 := |(S_1 - S_1^{\text{Haar}})/S_1^{\text{Haar}}|$ the relative gap with the Haar (Page) value. We see that for $g = 0$ (SYK4) the GS is closer than $g = 1$ (SYK2) to the Haar value, although none of them reaches the universal value. On the contrary, for MS, the relative gap shows a perfect adherence of SYK4 with Haar value unlike SYK2 as it is shown by the finite-size scaling in the inset. The behavior with g suggests that the MS universal properties are valid for all $g \neq 1$, making SYK4 robust from this point of view. A similar analysis has been conducted for SYK4 in [12].

A finer probe into the structure of entanglement is given by the full distribution of the eigenvalues of the RDM as we are focused on the half-subsystem. The reference Haar value is related to the Marchenko-Pastur (M-P) distribution as the limiting distribution of eigenvalues of Wishart matrices and reads $\eta^{\text{Haar}}(x) = 1 -$

$\frac{2}{\pi}(x\sqrt{1-x^2} + \arcsin x)$; see [38, 61]. To distinguish two probability distributions we employ the Kullback-Leibler divergence $D_{KL}(p||q) := \sum_i p_i(\log p_i - \log q_i)$. The results in the top row of Fig. 3 show the *fidelity* $D_{KL}(\eta_g|\eta_{g+\epsilon})$ between two distributions of the eigenvalues of the RDM for two nearby values $g, g + \epsilon$ of the interpolation parameter. This quantity can serve as a probe of a sharp transition associated with an observable consisting of a probability distribution. We see that the GS and MS behave in symmetric and opposite ways. The structure of the eigenvalues of the RDM of the GS shows a sharp transition at $g > 0$ and then smooths out. On the other hand, for the MS, $g = 1$ is fragile and the eigenvalues of the RDM of highly excited states are smoothly varying all the way as long as SYK4 interactions are different from zero. In the second row of Fig. 3 shows the same statistical distance between the state for the value g and the reference Haar value. While SYK4 is converging to the Haar value, SYK2 shoots away. The robustness of the two phases for GS and MS respectively is confirmed. In other words, for every value of $g \neq 1$, the eigenvalues of the RDM of highly excited states obey the universal Haar behavior.

Entanglement Spectrum Statistics (ESS).— Complex pattern of entanglement is characterized by universal properties of the statistics of the gaps in the entanglement spectrum, the so-called *entanglement spectrum statistics* (ESS) [44]. While chaotic systems, for instance, non-integrable systems obeying the eigenstate thermalization hypothesis (ETH) feature a universal, Wigner-Dyson (WD) behavior for the ESS, integrable, free-fermion models feature Poisson, while MBL states changes from WD in polynomial time after a quantum

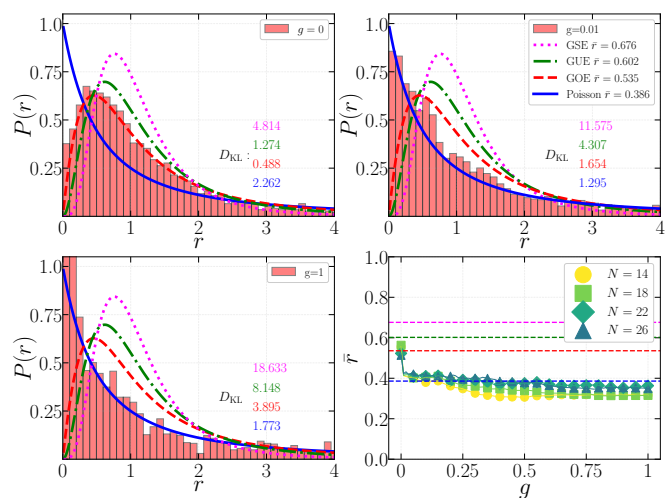


FIG. 4. ESS of the GS RDM eigenvalues of the H_g model for different values of g . We superimpose the analytical curves for the Wigner-Dyson (dashed) and Poisson (blue continuous) distribution for comparison. System size $N = 22$ and number of realizations is $M = 100$. The number of bins used for the histogram is 100. The colored numbers represent the KL divergence of data against known distributions [62]

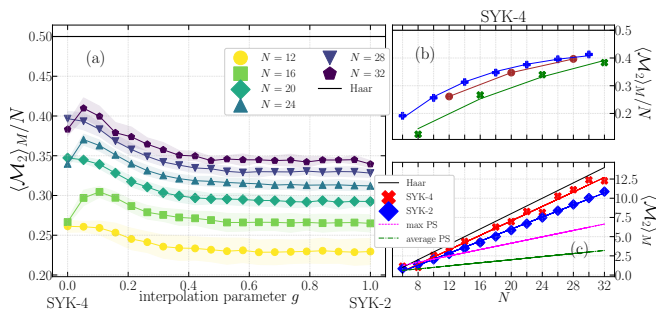


FIG. 5. Ensemble averaged SRE \mathcal{M}_2 in the GS of the interpolated SYK model. *Panel (a)*: For all g the ground states exhibit a non-vanishing amount of non-stabilizerness. *Panel (b)*: The non-monotonicity can be easily captured by a grouping of points according to: green crosses for $N \bmod 8 = 0$, blue crosses for $N \bmod 8 = 2, 6$, and red circles for $N \bmod 8 = 4$. The lines represent fits [60]. *Panel (c)*: SRE without the normalization with the system size as compared to the Haar value. PS here stands for the Product state [60].

quench [40]. The transition between the two regimes is due to the injection of non-stabilizer resources, which need to be scrambled around [39, 63].

From the perspective of random matrix theory, if the eigenvalues of the reduced density matrix are uncorrelated, the distribution is Poissonian. Conversely, correlated eigenvalues follow the Wigner-Dyson universality class. This observation underscores that the entanglement patterns between the two interpolating regimes exhibit differing complexities. We focus on the probability density function (PDF) of the consecutive spacing ratios denoted as $P(r)$. To evaluate it we use the ascending eigenvalues $\{\lambda_k\}$ of the reduced density matrix and determine the spacing ratio as $r_k = \frac{\lambda_{k+1} - \lambda_k}{\lambda_k - \lambda_{k-1}}$, where $k = 2, 3, \dots, 2^R - 1$. The resulting ratios $\{r_k\}$ are plotted as a normalized histogram, excluding rare outliers with $r_j > 10.0$ to ensure proper normalization and accurate binning [64, 65]. The explicit functional forms of the corresponding Poisson and Wigner-Dyson Gaussian ensembles are provided in [62]. To complement this type of analysis, we also evaluate the averaged consecutive spacing ratio, defined as $\bar{r} = \langle \langle \frac{\min(s_{k,j}, s_{k+1,j})}{\max(s_{k,j}, s_{k+1,j})} \rangle \rangle_{2^R-2, M}$ where the spacings are given by $s_{k,j} = \lambda_{k+1,j} - \lambda_{k,j}$, and the index $j = 1, 2, \dots, M$ refers to the different reduced density matrices considered across ensemble or disorder realizations.

In Fig. 4, we compute the ESS $P(r)$ for several values of the GS of the SYK4+SYK2 H_g model for several values of g . SYK4 ($g = 0$) adheres to the universal WD distribution for GOE as it is expected for a real Hamiltonian. As soon as the model is perturbed by SYK2, the distribution starts getting closer to Poisson. In the lower right panel, we show the behavior of the averaged consecutive spacing ratio \bar{r} as a function of g , which shows a sudden jump as one moves from $g = 0$. We can see that this

feature of the entanglement complexity which is typical of chaotic systems is fragile in the model. Similar results hold for the MS, see [60].

Stabilizer Rényi Entropy (SRE)— Non-stabilizerness is an essential property for universal quantum computation [66]. To quantify this property, we use the Stabilizer Rényi Entropy (SRE) [67], defined as

$$\mathcal{M}_\alpha(\Psi) = \frac{1}{1-\alpha} \log_2 \left(d^{-1} \sum_{P \in \mathcal{P}_N} |\text{Tr}(\Psi P)|^{2\alpha} \right). \quad (10)$$

Here, Ψ is the density matrix of an N -qubit state $|\Psi\rangle$, $d = 2^N$ is the Hilbert space dimension, and \mathcal{P}_N is the set of Pauli strings build from Pauli operators I, X, Y, Z . SREs for $\alpha \geq 2$ act as resource monotones but lack strong monotonicity [68]. Stabilizer entropies measure how far a state deviates from stabilizer states by analyzing its spread in the Pauli operator basis [67, 69]. The SRE stands out among non-stabilizerness monotones as it can be efficiently evaluated without the need for minimization procedures. In this work, we adopt the methodology outlined in Ref. [59] to compute the SRE. Specifically, we transform the ground state vectors obtained from exact diagonalization into matrix product state (MPS) tensor representations and employ the Perfect Sampling algorithm [70, 71].

In Fig. 5, we show the numerical results for the scaling of SRE in the GS of the H_g model. From panel (a), we observe that the SYK-4 ($g = 0$) case exhibits a higher degree of non-stabilizer resources compared to the SYK-2 ($g = 1$) limit. From Fig. 5 (a), we observe that the SRE of the SYK-4 ground states does not exhibit a consistent monotonic increase with fermion number N , but instead shows a non-monotonic dependence. A more detailed analysis in Fig. 5 (b) reveals an oscillatory pattern in the SRE. The data is grouped and labeled according to the values of $N \bmod 8$, as indicated in the captions. Each of the three groups corresponds to a distinct exponent of the damped exponential. This grouping is motivated by the observation in [72], where it was first noted that the SYK-4 Hamiltonian exhibits a particular particle-hole symmetry. The authors linked this symmetry to different Gaussian random matrix universality classes: GOE for $N \bmod 8 = 0$, GUE for $N \bmod 8 = 2, 6$, and GSE for $N \bmod 8 = 4$, which manifest in the Hamiltonian's spectrum. We observe the effects of this symmetry specifically in the ground state, without considering the full Hamiltonian spectrum. In contrast to entanglement (see Fig. 2) and ground state energy [73], the SRE appears to be much more sensitive to the finiteness of N . This highlights the unique ability of SRE to reveal hidden structures within many-body systems. A recent, striking example is the ability of SRE to detect a quantum phase transition that is not captured by entanglement in a system without a conventional order parameter [74].

How does the average SRE evolve as the system size increases for the ground state of the SYK-4 Hamiltonian?

This behavior is depicted in panel (c) of Fig. 5. By fitting the data to a linear function [75], we obtain the following expression for the average SRE:

$$\langle \mathcal{M}_2 \rangle_M^{\text{fit}} \sim -2.4 + 0.95 \frac{N}{2}. \quad (11)$$

For Haar random states, it is known that

$$\mathcal{M}_2^{\text{Haar}} = -2 + \frac{N}{2}, \quad (12)$$

to leading order in the system size [59, 67]. The factor of 2 in the denominator of the linear term arises because $N/2$ represents the support of the spin/qubit representation. Our results show that the SYK-4 ground states slightly deviate from the characteristics of fully quantum chaotic and universal states, with a linear prefactor difference of approximately 0.05 when compared to Haar random states. A similar deviation was recently observed in the entanglement of middle-of-the-spectrum states in the SYK-4 model [12]. This provides evidence that low-temperature states, such as the ground states, fail to reach full universality.

Anti-Flatness.— A crucial point in the understanding of the relationship between SRE and entanglement comes from the realization that stabilizer states must have a flat entanglement spectrum [76]. Indeed, one can show that there is a strict relationship between the lack of flatness of the entanglement spectrum of the RDM and the SRE of the full state. In [77] it is shown that the linear SRE is exactly proportional to the average anti-flatness defined on a subsystem as $\mathcal{F} := \text{Tr}[\rho_R^3] - \text{Tr}^2[\rho_R^2]$. Another measure of anti-flatness is a numerically and analytically accessible version of the anti-flatness quantity is the logarithmic anti-flatness [59]

$$F(\rho_R) := 2(S_2(\rho_R) - S_3(\rho_R)). \quad (13)$$

In Supplementary Material [60], an excellent agreement across all system sizes is observed with the analytical results we derive for the SYK2 ($g = 1$) limit where we obtained a closed-form expression for the logarithmic anti-flatness

$$F^{\text{SYK2}}(R, f) = 2R(1-f) \sum_{n=1}^{\infty} \frac{1}{n} \left(\frac{1}{2^n} - \frac{1}{2} \frac{3^n}{4^n} \right) \times {}_2F_1\left(\frac{1}{2}, 1-n, 2, 4f(1-f)\right) \quad (14)$$

where ${}_2F_1(a, b, c, d)$ is a hypergeometric function, $n > 0$, and $0 < f \leq 1/2$. For Haar random state in the large N limit the logarithmic anti-flatness approach system-size-independent value of $F^{\text{Haar}} = \log(5/4) \approx 0.223$ [59].

One of the most useful measures of anti-flatness comes from the modular entropy [78]

$$\tilde{S}_\alpha := \alpha^2 \partial_\alpha \left(\frac{\alpha-1}{\alpha} S_\alpha \right). \quad (15)$$

Its derivative with respect to the Rényi parameter at $\alpha = 1$ is minus the variance of the entanglement Hamiltonian

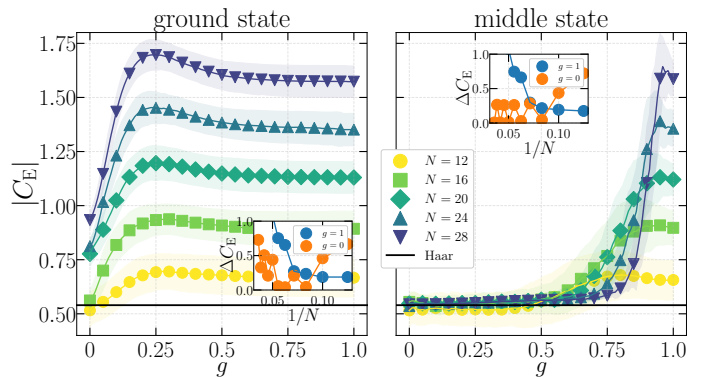


FIG. 6. Ensemble averaged half-system capacity of entanglement in the ground states (left panel) and in the middle of the state (right panel) of the interpolated SYK model. The inset shows how the relative gap defined as $\Delta C_E = |(C_E - C_E^{\text{Haar}})/C_E^{\text{Haar}}|$ of $g = 0$ (SYK4) and $g = 1$ (SYK2) scales with respect to the Haar value.

$H_\rho := -\log \rho$ defined as

$$-\text{Var}_\rho(H_\rho) := -\langle \log^2 \rho \rangle_\rho + \langle \log \rho \rangle_\rho^2 = \partial_\alpha \tilde{S}_\alpha \Big|_{\alpha=1} \quad (16)$$

and is also known as capacity of entanglement C_E [79–81]. This quantity is relevant because it quantifies the amount of non-local SRE, that is, the SRE that cannot be undone by local unitary operations [31]. For Haar random states, one can compute [82, 83]

$$\partial_\alpha \tilde{S}_\alpha^{\text{Haar}} \Big|_{\alpha=1} = \frac{11}{4} - \frac{\pi^2}{3} \approx -0.539868. \quad (17)$$

which we use in our analysis.

In Fig. 6, we compute the capacity of entanglement C_E as a probe of non-local SRE as a function of g in both the GS and MS of H_g . We see that SYK4 features a Haar-value capacity of entanglement, which is in perfect agreement in the MS. The finite-size scaling of the inset shows again the symmetric behavior of robustness observed earlier: while for the GS the SYK4 features are fragile, they are robust and can be extended all the way for any $g < 1$ for the MS.

Conclusions and Outlook.— In this paper, we studied the interplay between entanglement and non-stabilizer resources in the SYK4+SYK2 model through several figures of merit that involve probes into the non-local character of stabilizer entropy, the entanglement spectrum statistics, and the adherence of such quantities to predictions from random matrix theory. We show that SYK4 features a complex pattern of this interplay while the integrable SYK2 is not universal. Moreover, we show the robustness of the universal features of SYK4 and find that they vary greatly between the ground state and highly excited states. For this reason, it would be interesting to study the behavior of such interplay away from equilibrium and its role in operator scrambling [84].

Acknowledgments.— Upon completion of this paper, we stumbled onto arXiv:2502.01582 which has a simi-

lar scope with our work. An early version of our work was presented at the poster session of the first workshop on many-body quantum magic (MBQM2024), TII Abu Dhabi in November 2024: *Barbara Jasser, Chaos, Entanglement and Stabilizer Entropy in SYK model*. AH and JO acknowledge support from the PNRR MUR project PE0000023-NQSTI. AH acknowledges support from the PNRR MUR project CN 00000013-ICSC. This

work has been funded by project code PIR01 00011 ‘IBISCo’, PON 2014-2020, for all three entities (INFN, UNINA and CNR). Additionally, acknowledge ISCRA for awarding this project access to the LEONARDO supercomputer, owned by the EuroHPC Joint Undertaking, hosted by CINECA (Italy) under the project ID: PQC - HP10CQQ3SR We acknowledge stimulating conversations with P. Zanardi.

-
- [1] S. Sachdev and J. Ye, Physical review letters **70**, 3339 (1993).
- [2] KITP, Proceedings of the kitp (2015), <http://online.kitp.ucsb.edu/online/entangled15/kitaev/>, <http://online.kitp.ucsb.edu/online/entangled15/kitaev2/>.
- [3] D. Chowdhury, A. Georges, O. Parcollet, and S. Sachdev, Reviews of Modern Physics **94**, 035004 (2022).
- [4] A. Kitaev, Entanglement in strongly-correlated quantum matter , 38 (2015).
- [5] G. Sárosi, arXiv preprint arXiv:1711.08482 (2017).
- [6] D. A. Trunin, Physics-USpekhi **64**, 219 (2021).
- [7] J. Maldacena, S. H. Shenker, and D. Stanford, Journal of High Energy Physics **2016**, 1 (2016).
- [8] N. Tsuji and P. Werner, arXiv preprint arXiv:1812.04217 (2018).
- [9] Y. Gu, A. Kitaev, and P. Zhang, Journal of High Energy Physics **2022**, 1 (2022).
- [10] A. V. Lunkin, A. Y. Kitaev, and M. V. Feigel’man, Phys. Rev. Lett. **125**, 196602 (2020).
- [11] A. M. García-García, B. Loureiro, A. Romero-Bermúdez, and M. Tezuka, Physical review letters **120**, 241603 (2018).
- [12] Y. Huang, Y. Tan, and N. Y. Yao, Deviations from maximal entanglement for eigenstates of the sachdev-ye-kitaev model (2024), arXiv:2409.07043 [hep-th].
- [13] W. Fu and S. Sachdev, Physical Review B **94**, 035135 (2016).
- [14] C. Liu, X. Chen, and L. Balents, Physical Review B **97**, 245126 (2018).
- [15] P. Zhang, Frontiers of Physics **17**, 43201 (2022).
- [16] J. S. Cotler, G. Gur-Ari, M. Hanada, J. Polchinski, P. Saad, S. H. Shenker, D. Stanford, A. Streicher, and M. Tezuka, Journal of High Energy Physics **2017**, 1 (2017).
- [17] V. Veitch, S. A. Hamed Mousavian, D. Gottesman, and J. Emerson, New Journal of Physics **16**, 013009 (2014).
- [18] P. W. Shor, Physical review A **52**, R2493 (1995).
- [19] A. R. Calderbank and P. W. Shor, Physical Review A **54**, 1098 (1996).
- [20] C. H. Bennett, D. P. DiVincenzo, J. A. Smolin, and W. K. Wootters, Physical Review A **54**, 3824 (1996).
- [21] E. Knill and R. Laflamme, Physical Review A **55**, 900 (1997).
- [22] D. Gottesman, *Stabilizer codes and quantum error correction* (California Institute of Technology, 1997).
- [23] P. W. Shor, Proceedings of 37th conference on foundations of computer science (1996).
- [24] D. Gottesman, Physical Review A **57**, 127 (1998).
- [25] A. Y. Kitaev, Annals of physics **303**, 2 (2003).
- [26] E. T. Campbell, B. M. Terhal, and C. Vuillot, Nature **549**, 172 (2017).
- [27] L. Leone, S. F. Oliviero, and A. Hamma, Physical Review Letters **128**, 050402 (2022).
- [28] C. E. Robin and M. J. Savage, arXiv preprint arXiv:2405.10268 (2024).
- [29] F. Brökemeier, S. M. Hengstenberg, J. W. Keeble, C. E. Robin, F. Rocco, and M. J. Savage, arXiv preprint arXiv:2409.12064 (2024).
- [30] I. Chernyshev, C. E. Robin, and M. J. Savage, arXiv preprint arXiv:2411.04203 (2024).
- [31] C. Cao, G. Cheng, A. Hamma, L. Leone, W. Munizzi, and S. F. E. Oliviero, Gravitational back-reaction is magical (2024), arXiv:2403.07056 [hep-th].
- [32] S. F. E. Oliviero, L. Leone, and A. Hamma, Physical Review A **106**, 042426 (2022).
- [33] C. D. White, C. Cao, and B. Swingle, Phys. Rev. B **103**, 075145 (2021).
- [34] R. Nyström, N. Pranzini, and E. Keski-Vakkuri, arXiv preprint arXiv:2409.11473 (2024).
- [35] S. Cepollaro, S. Cusumano, A. Hamma, G. L. Giudice, and J. Odavic, arXiv preprint arXiv:2412.11918 (2024).
- [36] L. Leone, S. F. E. Oliviero, Y. Zhou, and A. Hamma, Quantum **5**, 453 (2021).
- [37] S. F. Oliviero, L. Leone, and A. Hamma, Physics Letters A **418**, 127721 (2021).
- [38] Z.-C. Yang, C. Chamon, A. Hamma, and E. R. Mucciolo, Physical review letters **115**, 267206 (2015).
- [39] S. Zhou, Z. Yang, A. Hamma, and C. Chamon, SciPost Physics **9**, 087 (2020).
- [40] Z.-C. Yang, A. Hamma, S. M. Giampaolo, E. R. Mucciolo, and C. Chamon, Physical Review B **96**, 020408 (2017).
- [41] M. Rigol, V. Dunjko, and M. Olshanii, Nature **452**, 854 (2008).
- [42] A. Pal and D. A. Huse, Physical Review B—Condensed Matter and Materials Physics **82**, 174411 (2010).
- [43] R. Nandkishore and D. A. Huse, Annu. Rev. Condens. Matter Phys. **6**, 15 (2015).
- [44] C. Chamon, A. Hamma, and E. R. Mucciolo, Physical Review Letters **112**, 240501 (2014).
- [45] D. Shaffer, C. Chamon, A. Hamma, and E. R. Mucciolo, Journal of Statistical Mechanics: Theory and Experiment **2014**, P12007 (2014).
- [46] A. Kitaev, in *Proceedings of the Stanford SITP seminars* (2014).
- [47] B. Kobrin, Z. Yang, G. D. Kahanamoku-Meyer, C. T. Olund, J. E. Moore, D. Stanford, and N. Y. Yao, Physical review letters **126**, 030602 (2021).
- [48] P. Orman, H. Gharibyan, and J. Preskill, arXiv preprint arXiv:2403.13884 (2024).
- [49] K. Adhikari and A. Bose, Random Matrices: Theory and

- Applications **9**, 2050002 (2020).
- [50] P. J. Forrester, *Journal of Physics A: Mathematical and General* **39**, 6861 (2006).
- [51] P. J. Forrester, J. R. Ipsen, and S. Kumar, *Experimental Mathematics* **29**, 276 (2020).
- [52] K. Zyczkowski and H.-J. Sommers, *Journal of Physics A: Mathematical and General* **33**, 2045 (2000).
- [53] S. B. Bravyi and A. Y. Kitaev, *Annals of Physics* **298**, 210 (2002).
- [54] P. H. C. Lau, C.-T. Ma, J. Murugan, and M. Tezuka, *Journal of Physics A: Mathematical and Theoretical* **54**, 095401 (2021).
- [55] P. Lydzba, M. Rigol, and L. Vidmar, *Physical review letters* **125**, 180604 (2020).
- [56] Y. Huang and Y. Gu, *Physical Review D* **100**, 041901 (2019), arXiv:1709.09160 [hep-th].
- [57] P. Zhang, C. Liu, and X. Chen, *SciPost Physics* **8**, 094 (2020).
- [58] D. N. Page, *Physical Review Letters* **71**, 1291–1294 (1993).
- [59] J. Odavić, M. Viscardi, and A. Hamma, Stabilizer entropy in non-integrable quantum evolutions (2024), arXiv:2412.10228 [quant-ph].
- [60] B. Jasser, J. Odavić, and A. Hamma, Supplementary material for “stabilizer entropy and entanglement complexity in the sachdev-ye-kitaev model” (2025).
- [61] W. Mück, *Phys. Rev. D* **109**, 126001 (2024).
- [62] Y. Y. Atas, E. Bogomolny, O. Giraud, and G. Roux, *Physical Review Letters* **110**, 084101 (2013).
- [63] S. True and A. Hamma, *Quantum* **6**, 818 (2022).
- [64] J. Odavić, G. Torre, N. Mijić, D. Davidović, F. Franchini, and S. M. Giampaolo, *Quantum* **7**, 1115 (2023).
- [65] J. Odavić and P. Mali, *Journal of Statistical Mechanics: Theory and Experiment* **2021**, 043204 (2021).
- [66] S. Bravyi and A. Kitaev, *Physical Review A* **71**, 022316 (2005).
- [67] L. Leone, S. F. Oliviero, and A. Hamma, *Physical Review Letters* **128**, 050402 (2022).
- [68] L. Leone and L. Bittel, Stabilizer entropies are monotones for magic-state resource theory (2024), arXiv:2404.11652.
- [69] P. Niroula, C. D. White, Q. Wang, S. Johri, D. Zhu, C. Monroe, C. Noel, and M. J. Gullans, *Nature Physics*, 1–7 (2024).
- [70] T. Haug and L. Piroli, *Quantum* **7**, 1092 (2023).
- [71] G. Lami and M. Collura, *Physical Review Letters* **131**, 10.1103/PhysRevLett.131.180401 (2023).
- [72] J. S. Cotler, G. Gur-Ari, M. Hanada, J. Polchinski, P. Saad, S. H. Shenker, D. Stanford, A. Streicher, and M. Tezuka, *Journal of High Energy Physics* **2017**, 118 (2017).
- [73] A. M. García-García and J. J. Verbaarschot, *Physical Review D* **94**, 126010 (2016).
- [74] A. G. Catalano, J. Odavić, G. Torre, A. Hamma, F. Franchini, and S. M. Giampaolo, Magic phase transition and non-local complexity in generalized w state (2024), arXiv:2406.19457 [quant-ph].
- [75] Z.-W. Liu and A. Winter, *PRX Quantum* **3**, 020333 (2022).
- [76] A. Hamma, R. Ionicioiu, and P. Zanardi, *Physical Review A—Atomic, Molecular, and Optical Physics* **71**, 022315 (2005).
- [77] E. Tirrito, P. S. Tarabunga, G. Lami, T. Chanda, L. Leone, S. F. Oliviero, M. Dalmonte, M. Collura, and A. Hamma, *Physical Review A* **109**, L040401 (2024).
- [78] X. Dong, A. Lewkowycz, and M. Rangamani, *Journal of High Energy Physics* **2016**, 28 (2016).
- [79] H. Yao and X.-L. Qi, *Physical review letters* **105**, 080501 (2010).
- [80] J. Schliemann, *Physical Review B—Condensed Matter and Materials Physics* **83**, 115322 (2011).
- [81] J. De Boer, J. Järvelä, and E. Keski-Vakkuri, *Physical Review D* **99**, 066012 (2019).
- [82] J. de Boer, J. Järvelä, and E. Keski-Vakkuri, *Physical Review D* **99**, 066012 (2019).
- [83] K. Okuyama, *Physics Letters B* **820**, 136600 (2021).
- [84] G. Styliaris, N. Anand, and P. Zanardi, *Phys. Rev. Lett.* **126**, 030601 (2021).